

Improvement of human embryonic stem cell-derived retinal pigment epithelium cell adhesion, maturation, and function through coating with truncated recombinant human vitronectin

Xin-Yue Zhu^{1,2,3,4}, Yu-Hong Chen^{1,2,3,4}, Ting Zhang^{1,2,3,4}, Su-Jun Liu^{1,2,3,4}, Xin-Yue Bai^{1,2,3,4}, Xian-Yu Huang^{1,2,3,4}, Mei Jiang^{1,2,3,4}, Xiao-Dong Sun^{1,2,3,4}

¹Department of Ophthalmology, Shanghai General Hospital, Shanghai Jiao Tong University School of Medicine, Shanghai 200080, China

²National Clinical Research Center for Eye Diseases, Shanghai 200080, China

³Shanghai Key Laboratory of Fundus Diseases, Shanghai 200080, China

⁴Shanghai Engineering Center for Visual Science and Photomedicine, Shanghai 200080, China

Co-first authors: Xin-Yue Zhu and Yu-Hong Chen

Correspondence to: Xiao-Dong Sun and Mei Jiang. Department of Ophthalmology, Shanghai General Hospital, Shanghai Jiao Tong University School of Medicine, 100 Hai Ning Road, Shanghai 200080, China. xdsun@sjtu.edu.cn; mei.jiang@shgh.cn

Received: 2021-01-06 Accepted: 2021-04-21

Abstract

• **AIM:** To explore an xeno-free and defined coating substrate suitable for the culture of H9 human embryonic stem cell-derived retinal pigment epithelial (hES-RPE) cells *in vitro*, and compare the behaviors and functions of hES-RPE cells on two culture substrates, laminin521 (LN-521) and truncated recombinant human vitronectin (VTN-N).

• **METHODS:** hES-RPE cells were used in the experiment. The abilities of LN-521 and VTN-N at different concentrations to adhere to hES-RPE cells were compared with a high-content imaging system. Quantitative real-time polymerase chain reaction was used to evaluate RPE-specific gene expression levels midway (day 10) and at the end (day 20) of the time course. Cell polarity was observed by immunofluorescent staining for apical and basal markers of the RPE. The phagocytic ability of hES-RPE cells was identified by flow cytometry and immunofluorescence.

• **RESULTS:** The cell adhesion assay showed that the ability of LN-521 to adhere to hES-RPE cells was dose-

dependent. With increasing coating concentration, an increasing number of cells attached to the surface of LN-521-coated wells. In contrast, VTN-N presented a strong adhesive ability even at a low concentration. The optimal concentration of LN-521 and VTN-N required to coat and adhesion to hES-RPE cells were 2 and 0.25 $\mu\text{g}/\text{cm}^2$, respectively. Furthermore, both LN-521 and VTN-N could facilitate adoption of the desired cobblestone cellular morphology with tight junction and showed polarity by the hES-RPE cells. However, hES-RPE cells cultivated in VTN-N had a greater phagocytic ability, and it took less time for these hES-RPE cells to mature.

• **CONCLUSION:** VTN-N is a more suitable coating substrate for cultivating hES-RPE cells.

• **KEYWORDS:** retinal pigment epithelial; stem cell; surface coating; laminin; vitronectin; cell adhesion; phagocytosis

DOI:10.18240/ijo.2021.08.04

Citation: Zhu XY, Chen YH, Zhang T, Liu SJ, Bai XY, Huang XY, Jiang M, Sun XD. Improvement of human embryonic stem cell-derived retinal pigment epithelium cell adhesion, maturation, and function through coating with truncated recombinant human vitronectin. *Int J Ophthalmol* 2021;14(8):1160-1167

INTRODUCTION

H9 human embryonic stem cell-derived retinal pigment epithelial (hES-RPE) cells, a potential cell source for cell transplantation therapy of retinal degenerative diseases, are especially useful in atrophic ‘dry’ age-related macular degeneration (AMD) and retinitis pigmentosa (RP). These retinal degenerative diseases are characterized by RPE damage, degeneration, loss and progressive cellular dysfunction of the neuroretina^[1-2]. A challenge in the clinical transformation of cell transplantation is to generate optimized hES-RPE cells on a large-scale to meet clinical use requirements and ensuring their quality, quantity, consistency, and safety *in vitro*^[3].

hES-RPE cell culture *in vitro* requires coating substrates to facilitate cell adhesion, growth, and mature, as they can affect cell integration and survival after cell transplantation^[4]. Previously devised systems have used complex and undefined substrates, such as feeder fibroblast layers or Matrigel. Matrigel is currently the conventional coating substrate for hES-RPE cell culture. However, Matrigel is extracted from the Engelbreth-Holm-Swarm (EHS) mouse sarcoma, a tumor rich in extracellular matrix (ECM) proteins, exhibits lot-to-lot variability and can introduce unwanted xenogeneic contaminants. Thus, the use of Matrigel is not safe for clinical transplantation^[5]. Therefore, there is a need to explore human recombinant cell culture matrix proteins as the coating substrates. Currently, the lack of xeno-free, defined coating substrates and standardized culture system has hampered the clinically application of functional and safe hES-RPE cells^[6].

To explore defined, purified ECM proteins as coatings, researchers have tried to use single ECM protein components as coating substrates. The effects of defined ECM proteins as coating substrates for human embryonic stem cell (hESC) differentiation or hES-RPE cell maintenance remain elusive, but important for clinical translation. It has been reported that multiple purified ECM proteins, such as synthemax II-SC^[7], collagens (I and IV)^[8], fibronectin^[8], and vitronectin^[9] in fully-defined, feeder-free culture systems support the growth of induced pluripotent stem cells (iPSCs), the differentiation of pigmented regions from iPSCs and the maintenance of iPSC-RPEs. Laminin521 (LN-521) is ubiquitous in human basement membranes and can support stem cells without feeder and rock inhibitor^[10]. To date, LN-521 is another promising ECM proteins for future clinical-grade coating substrates^[11-13]. A recent study had shown successfully RPE differentiation with preclinical efficiency using LN-521 matrix^[13]. LN-521-based RPE culture and differentiation methods are likely to find extensive use in generating therapeutic stem cell-derived RPE for regenerative medicine. However, evaluation of the effects of LN-521 on stem cell-derived RPE adhesion, maturation, and function after differentiation has not been performed yet. Vitronectin has been used to culture stem cell derived-RPE cells in many clinical trials so far^[1-2]. To the best of our knowledge, which coating substrates of those two is more conducive to hES-RPE cell culture has not been described. Hence, in the present study, we aimed to investigate the effect of LN-521 on hES-RPE adhesion, maturation, and function after differentiation, and compare it to vitronectin.

In this study, we selected commercially available human recombinant laminin cell culture matrices, LN-521 (one isoform of laminin) and truncated recombinant human vitronectin (VTN-N)^[14], to identify their adhesion ability for hES-RPE

cells, and their effects on the morphology, maturation and function of the cells *in vitro*. First, we verified the optimal coating concentrations of LN-521 and VTN-N for hES-RPE cell adhesion. As the first step in the interaction between cells and a material, cell adhesion seems to play a key role in cellular characteristics and determines the growth of the cells^[15-17]. This will be very helpful for establishing a standardized large-scale hES-RPE cell culture protocol. Furthermore, we evaluated the morphology, maturity, and phagocytic function of hES-RPE cells on both coating substrates. Our results demonstrated that hES-RPE on VTN-N matured more rapidly and showed better phagocytic ability. Taken together, our findings may serve as the basis for the future transplantation of healthy hES-RPE cells into the subretinal space for successful RPE functional repair^[8].

MATERIALS AND METHODS

LN-521/VTN-N Coating First, we calculated the stock solution concentrations and amounts of LN-521 (Biolamina, LN521) and VTN-N (Gibco, A14700) needed for the experiments and slowly thawed the coatings at 4°C before use. The LN-521 and VTN-N stock solutions were diluted with 1×dulbecco's phosphate-buffered saline (DPBS, with Ca²⁺ and Mg²⁺) and 1×DPBS (without Ca²⁺ and Mg²⁺) to different concentration (0, 0.25, 0.5, 1, 2, 4, 8 μg/cm²). For the dose-response adhesion assay, 96-well black glass bottom plates were used. For other experiments, we used 24-well plates and Millicell EZ Slide 4-well glass (Millipore, PEZGS0416). The dilute solutions were added to each culture vessel at the recommended volumes. The coated plates were incubated at 4°C overnight. Prior to use, the culture vessels were prewarmed to room temperature for at least 1h. LN-521 coated vessels needed to be rinsed with 1× DPBS (with Ca²⁺ and Mg²⁺) before use.

hES-RPE Cell Culture and Seeding H9 hESCs were spontaneously differentiated into RPE (hES-RPE) cells as described previously^[18]. hES-RPE cells were cultured with X-VIVO 10 medium for at least 30-35d at passage 1 and frozen at passage 2 on day 5^[19]. Cultures were free of mycoplasma as evaluated by polymerase chain reaction (PCR; data not shown). The hES-RPE cells were plated at a density of 1.0×10⁵ cells/cm² in culture medium. The cells were cultured at least 2-3wk in X-VIVO 10 media except for phagocytosis analyses, for which the cells were cultured in MEM-Nic medium^[20] [MEM alpha with GlutaMAX, 1% fetal bovine serum (FBS), 1% penicillin/streptomycin, 0.1 mmol/L non-essential amino acids (NEAA), 1% N1 supplement, 0.25 mg/mL taurine, 20 ng/mL hydrocortisone, 0.013 ng/mL triiodo-thyronin, and 10 mmol/L nicotinamide]. The cells were maintained at 37°C, 5% CO₂, and the medium was replaced with fresh medium three times per week.

Table 1 The sequence of primers used in the real-time PCR

Gene	GenBank number	Sequence
RPE65	NM_000329.3	Forward: 5'-GCCAATTTACGTGAGAACTGGG-3' Reverse: 5'-CCAGATAGTCTCGTCACTGCAC-3'
BEST1	NM_004183.4	Forward: 5'-CTGGGCTTCTACGTGACGC-3' Reverse: 5'-TTGCTCGTCCTTGCCTTCG-3'
TYR	NM_000372.5	Forward: 5'-TGCACAGAGAGACGACTCTTG-3' Reverse: 5'-GAGCTGATGGTATGCTTTGCTAA-3'
MITF	NM_001354604.2	Forward: 5'-ACTTTCACCTTCGCCAAGG-3' Reverse: 5'-TGCGTGATGCATACTGGAG-3'
PMEL	NM_006928.5	Forward: 5'-AGGTGCCTTTCTCCGTGAG-3' Reverse: 5'-AGCTTCAGCCAGATAGCCACT-3'
GAPDH	NM_002046.7	Forward: 5'-AGCACAAGAGGAAGAGAGAGACCC-3' Reverse: 5'-TGAGCACAGGGTACTTTATTGATGGTACATG-3'

Cell Adhesion Assay Dose-response adhesion assays were performed with a previously used protocol with some modifications^[9,21]. Briefly, hES-RPE cells were seeded into each well of 96-well plates coated with LN-521 and VTN-N at 1.0×10^5 cells/cm². After 6h of incubation, the nonadherent cells were removed by rinsing 3 times with $1 \times$ DPBS (with Ca²⁺ and Mg²⁺), and the adherent cells were fixed with 4% paraformaldehyde (PFA) for 15min at room temperature. Cells were then stained with DAPI for 10min at room temperature. The cells were quantified and analyzed with a high content imaging system (PE, Operetta).

Quantitative Real-time Polymerase Chain Reaction

Cells were collected and total RNA was isolated using the RNAsimple Total RNA Kit (Tiangen, DP419). cDNA was synthesized from 500 ng of total RNA using PrimeScript RT Master Mix (Takara, Japan, RR0036A). TB Green Fast qPCR Mix (Takara) and the ViiA7 real-time PCR system (Thermo Fisher) were used to perform quantitative real-time polymerase chain reaction (qRT-PCR). The primer sequences used for qRT-PCR are shown in Table 1. Triplicate reactions were run in a 96-well plate for each sample. Cycle threshold (Ct) values were obtained from the thermal cycler, and $2^{-\Delta\Delta Ct}$ was calculated to determine the expression level of target genes.

Immunofluorescent Staining The hES-RPE cells were cultured for 20d after being plated on Millicell EZ Slide 4-well glass coated with Matrigel, LN-521 or VTN-N. The cells were fixed with 4% PFA for 15min at room temperature and then permeabilized with 50% ethanol for 5min at room temperature. After washing 3 times with blocking buffer (5% goat serum, 0.5% BSA and 0.05% saponin in PBS), the cells were incubated with primary antibody in blocking buffer overnight at 4°C. Primary antibodies against the following were used for immunostaining: ZO1 (Invitrogen, 33-9100; 1:200), BEST1 (Abcam, ab2182; 1:1000), phalloidin-iFluor488 (Abcam, ab176753; 1:1000), and phalloidin-iFluor647 (Abcam, ab176759; 1:1000). Then, the cells were washed 3 times with

blocking buffer and incubated with Alexa Fluor-conjugated secondary antibodies for 1h at room temperature. Nuclei were stained with DAPI. Images were taken using a confocal microscope (Leica, DMI8).

Isolation of Photoreceptor Outer Segments

Photoreceptor outer segments (POS) were isolated from fresh porcine eyes according to established protocols with minor modifications^[22]. Briefly, set up continuous sucrose gradients (27%-50%) in ultra-clear centrifuge tubes before the procedure and keep on ice until ready to use. Each gradient is 22 mL in volume and can hold a maximum of 8 retinas. Then, detached the retinas and homogenized with glass homogenizer, spin at 1000 RPM for 3min. Collect the supernatants and add a maximum of 4 mL to each gradient. Spin at 24000 RPM in a SW40-Ti rotor for 1h and 10min at 4°C. At the end of the run, there should be 3 bands on the gradient. The middle band is orange and contains most of the POS. Quickly mark and draw up everything in the middle orange band only and transfer to a new tube. Dilute the mixture with isolation medium and spin at 9500 RPM for 10min at 4°C. There should be an orange pellet off to the side of the tubes. Decant the supernatant and suspend the POS in DEME medium with 2.5% sucrose to determine the yield under the hemocytometer or store at -80°C for future use.

Phagocytosis Assay and Flow Cytometry Analysis

A phagocytosis assay was performed as previously described with some modifications^[18]. Briefly, hES-RPE cells were seeded on Matrigel, LN-521 and VTN-N coated plates at a density of 1.0×10^5 cells/cm² and cultured in MEM-Nic medium for at least 20d until the RPE cells reached confluence. Prelabeled (AlexaFluor 555/647 NHS Ester, Invitrogen, A20109/A20006) POS were added to the hES-RPE cells (10 POS/per cell) and incubated for 4h at 37°C in 5% CO₂. The cells were vigorously washed 5 times with $1 \times$ DPBS (with Ca²⁺ and Mg²⁺) to remove unbound POS. Images were captured by fluorescence microscopy. The phagocytic ability of hES-RPE cells coated with different substrates was also be

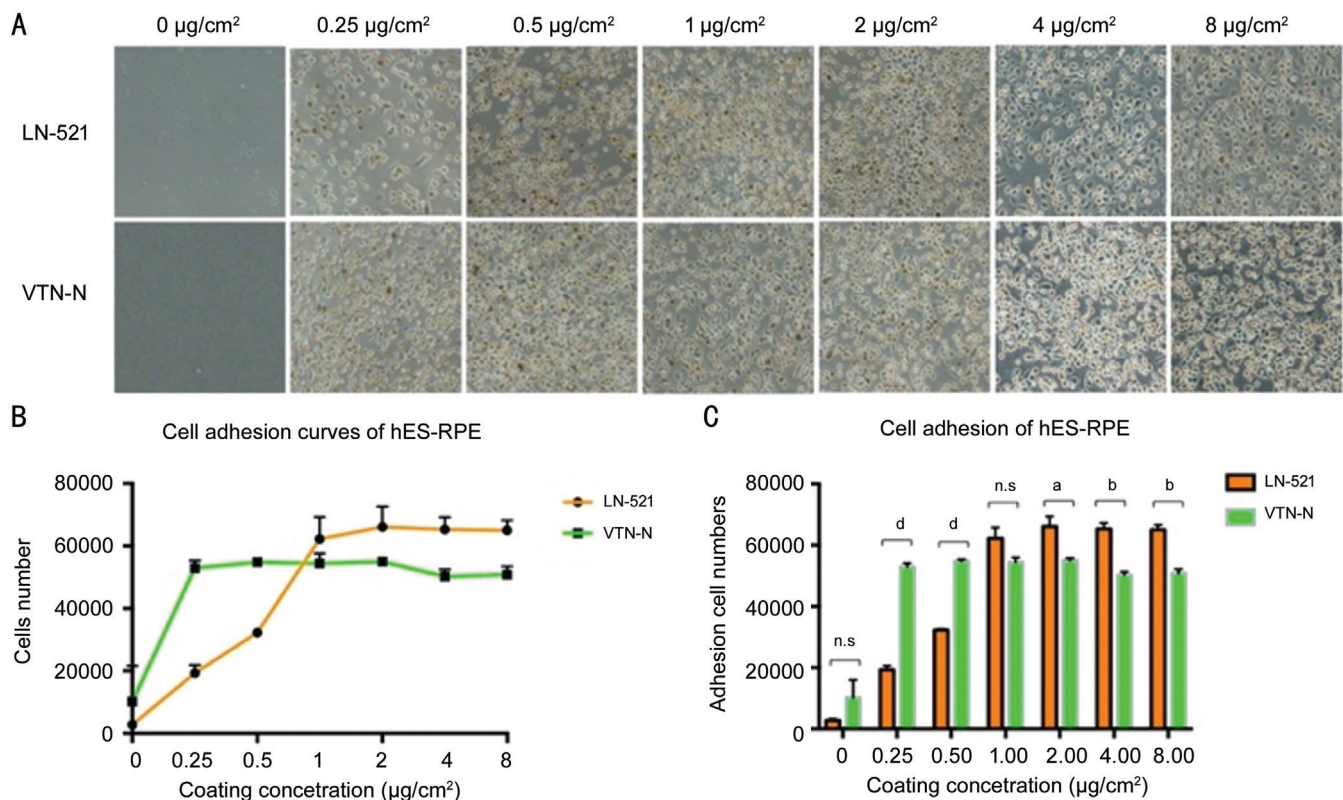


Figure 1 hES-RPE cell adhesion on LN-521 and VTN-N. A: Brightfield images of hES-RPE cells adhered to LN-521 and VTN-N coated wells after 6h of incubation with different concentrations (0, 0.25, 0.5, 1, 2, 4, and 8 µg/cm²). B: Cells were quantified and analyzed with a high content imaging system. The number of adhesion cells on LN-521 increased until reaching the optimal concentration 2 µg/cm², while cell adhesion on VTN-N was not significantly different from the concentration of 0.25 µg/cm². C: Comparison of the number of cells with the two coating substrates at each concentration tested. Unpaired *t*-tests were performed. ^a*P*<0.05, ^b*P*<0.01, ^d*P*<0.0001.

identified by flow cytometry. After incubation with pre-labeled (AlexaFluor647) POS for 4h at 37°C in 5% CO₂ and complete washing, the cells were harvested with TrypLE Select Enzyme (1×, Thermo Fisher) and resuspended in PBS to produce a single-cell suspension. A FACS scan flow cytometry machine (Beckman Coulter, CytoFLEX) was used to measure the AlexaFluor647 fluorescence-positive cells.

Statistical Analysis All results presented were obtained from at least three times independent experiments. GraphPad Prism 7 was used for mapping and statistical analyses. The results are presented as the average value±SD. Differences were considered statistically significant if the *P* value<0.05.

RESULTS

Comparison of Adhesion of hES-RPE Cells on LN-521 and VTN-N In investigating the adhesion of LN-521 and VTN-N to hES-RPE cells, we found that LN-521 and VTN-N can both enhance cell adhesion. After 6h of incubation, very few hES-RPE cells adhered to wells without a coating. With increasing coating concentration, increasing numbers of cells attached to the surface of the coated wells (Figure 1A). As shown in Figure 1B, the optimum concentration of LN-521 for hES-RPE cell adhesion was 2 µg/cm². When the concentration exceeded 2 µg/cm², there was no significant increase in cell

attachment. However, VTN-N at a concentration of only 0.25 µg/cm² already showed good hES-RPE cell adhesion, and with increasing concentration, the number of attached cells did not obviously increase. In addition, when the coating concentration was less than 1 µg/cm², the adhesion of VTN-N to the cells was significantly better than that of LN-521 (*P*<0.05), however, when the coating concentration was higher than 1 µg/cm², the total number of hES-RPE cells adhered to the LN-521 was superior to that of cells adhered to VTN-N (*P*<0.05; Figure 1C). The optimal concentrations of LN-521 and VTN-N for hES-RPE cell adherence were 2 and 0.25 µg/cm², respectively, which is inconsistent with the manufacturers' recommendations (0.5 µg/cm² for LN-521; 0.9 µg/cm² for VTN-N). This result will be very valuable for the culture of hES-RPE cells under the best conditions and at the lowest cost.

Impact of LN-521 and VTN-N on Cell Morphology and Polarity of hES-RPE To evaluate hES-RPE cell maturity, we compared the cell morphology and polarity of hES-RPE cells on LN-521, VTN-N, and Matrigel. Three kinds of substrates all induced a cobblestone-like morphology in the hES-RPE cells, which showed evidence of tight junctions at approximately 2-3wk after seeding (Figure 2A). RPE cell function is closely related to cell polarity. Cell polarity at day

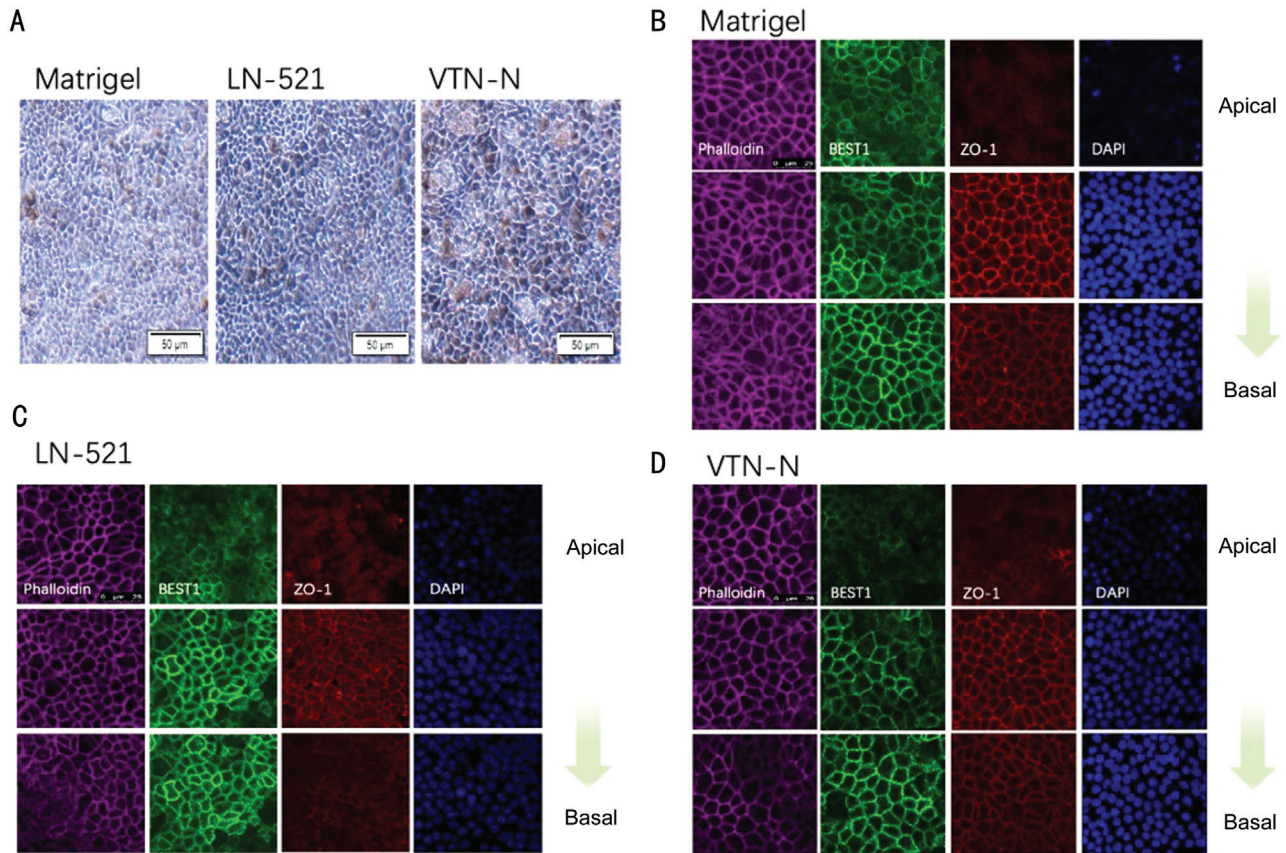


Figure 2 Morphology and protein localization in hES-RPE cells on Matrigel, LN-521, and VTN-N A: Brightfield image of cultured passage 3 hES-RPE cells under a 20× objective on day 20; B: Matrigel; C: LN-521; D: VTN-N. hES-RPE cells express properly localized apical phalloidin (purple), basal BEST1 (green) and ZO-1 (red) at tight junctions. Scale bars: 25 µm.

20 was assessed by immunostaining for F-actin, an apical marker^[23-24], basal marker BEST1^[25], and tight junction marker, ZO-1. hES-RPE cells grown on the three kinds of coating substrates had predominantly apical expression of F-actin (purple, phalloidin) and basal expression of BEST1 (green), indicating polarization (Figure 2B-2D). Also those cells all showed strong ZO-1 staining, which was highly visible at the margins of the hexagonally shaped RPE cells (Figure 2B-2D, red). These results revealed that the coating substrates LN-521 and VTN-N were suitable to support hES-RPE cell polarity and maturity, at least at the optimum coating concentration and with sufficient cultivation time.

Effect of LN-521 and VTN-N on RPE Maturation After Passage An examination of gene expression in hES-RPE cells was performed by qPCR analysis. We evaluated and compared gene expression levels with the two coating substrates relative to those with Matrigel midway (day 10) and at the end (day 20) of the experimental time course. Expression levels of the RPE-specific markers, retinal pigment epithelium specific protein 65 (RPE65)^[26], bestrophin1 (BEST1, a calcium-activated chloride channel)^[25], melanin-producing tyrosinase (TYR)^[27], microphthalmia-associated transcription factor (MITF)^[28] and premelanosome protein (PMEL)^[29] were evaluated. As shown

in Figure 3, all of these RPE-specific markers were expressed at higher levels in the VTN-N group than in the LN-521 group on day 10. However, the expression of these markers did not significantly differ between the two substrates groups on day 20. This result suggests that hES-RPE cells cultured on VTN-N substrate matured and showed RPE characteristics faster than those cultured on LN-521.

Abilities of LN-521 and VTN-N to Affect RPE Phagocytosis

The phagocytic abilities of hES-RPE cells cultured on the coating substrates Matrigel, LN-521, and VTN-N were compared to further verify the cell function. After incubation with pre-labeled POS for 4h at 37°C in 5% CO₂, total POS (red) bound and ingested by hES-RPE cells cultured on different coating substrates was detected, as shown in Figure 4A. Phalloidin-iFluor 488 (green) was used to show the apical zone of the cells. Flow cytometry analysis also showed that 93.4%, 96.5%, 98.2% of hES-RPE cells on Matrigel, LN-521, and VTN-N respectively were POS-positive (Figure 4B). At this stage, more than 78.15% of the total POS were bound POS (data not shown). Based on that, the difference in the total amount of phagocytosed POS were from bound POS not ingested POS. Therefore, this result indicated that hES-RPE cells on the VTN-N presented the highest phagocytic activity.

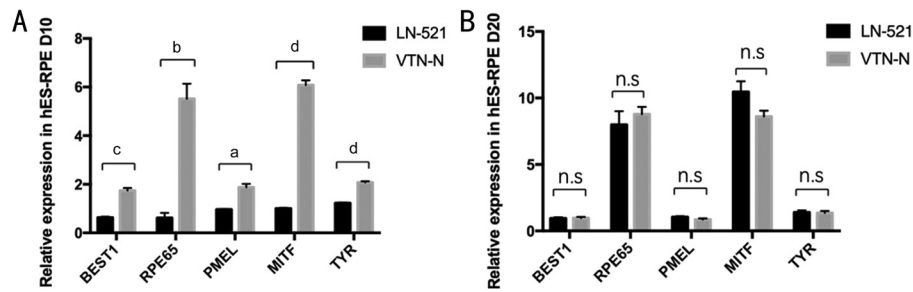


Figure 3 Gene expression in hES-RPE cells on days 10 and 20 qPCR analysis was carried out to compare gene expression levels in hES-RPE cells cultured on LN-521 or VTN-N relative to those cultured on Matrigel as a control at day 10 (A) and day 20 (B). Unpaired *t*-tests were performed. ^a*P*<0.05, ^b*P*<0.01, ^c*P*<0.001, ^d*P*<0.0001.

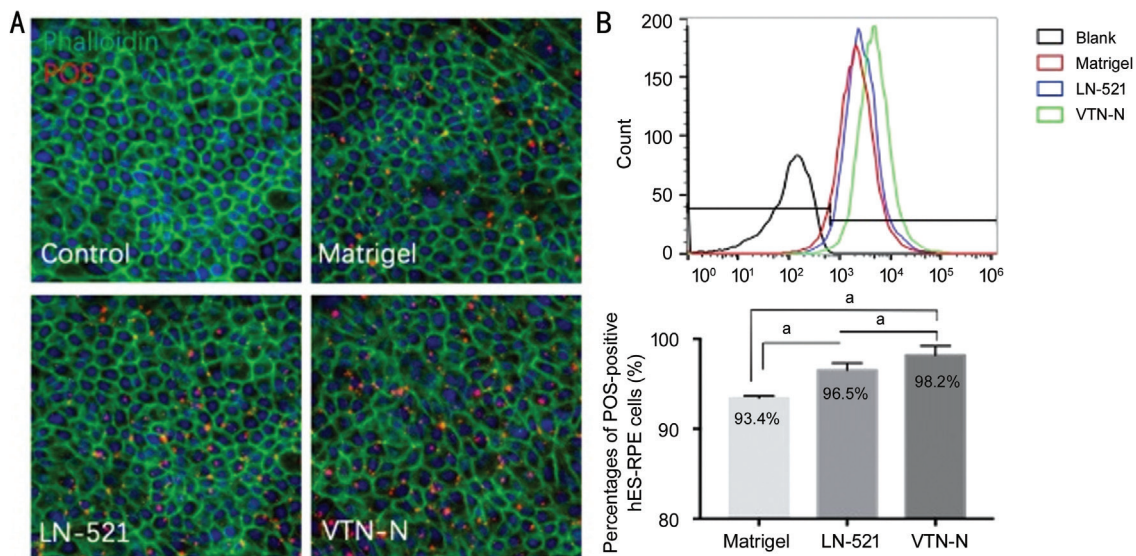


Figure 4 VTN-N coated hES-RPE cells bind more POS than Matrigel or LN-521 coated hES-RPE cells A: Prelabeled (AlexaFluor555) POS (red) were bound to hES-RPE cells. Immunofluorescent staining with phalloidin-iFluor 488 showed a cobblestone-like cellular morphology. B: Flow cytometry analysis showed that the percentages of POS-positive hES-RPE cells on Matrigel, LN-521, and VTN-N were 93.4%, 96.5%, 98.2% respectively. Paired *t*-tests were performed (^a*P*<0.05).

In addition, with both LN-521 and VTN-N, the fluorescence intensity of combined POS was greater than that with Matrigel. This result suggests that a defined coating substrate is more effective than undefined complex substrates.

DISCUSSION

Stem cell-based therapy is a promising therapeutic treatment for late-stage AMD, which is one of the leading causes of blindness. Multiple phase I/II clinical trials for stem cell-based therapies primarily designed to examine the safety of stem cell-derived RPE transplantation in late-stage AMD have begun^[30-32]. However, the quality of the transplanted hES-RPE cells is very important for long-term survival and function after transplantation. While Matrigel has been a very common ECM for stem cell-based RPE differentiation and culture, it is critical to establish an alternative ECM substrate, which is animal-free and non-xenogenic for cell therapy development and clinical trials. Two of the most popular defined matrices routinely employed in hES-RPE culture are laminin and vitronectin^[33-34]. In this study, we provide the first comprehensive analysis of

those two substrates (LN-521 and VTN-N) on cell adhesion, morphology, polarity and phagocytic function of hES-RPE cells. The results showed that the adhesion of LN-521 to the cells was dose-dependent, however, VTN-N presented a good adhesive ability even at low concentrations. This indicates that the ability of VTN-N to adhere to hES-RPE cells is relatively stable and that VTN-N is less affected by changes in concentration or batch-to-batch variation than LN-521. It is very important for industrial Good Manufacturing Practice (GMP) production to maintain good stability and quality. The low concentration of the coating VTN-N needed and its high stability for cell adhesion will be the significant advantages for the large-scale industrial production of hES-RPE cells for future clinical applications. Although the number of adherent cells in the LN-521 group was slightly greater than that in the VTN-N group when the coating concentration was above 2 μg/cm², this difference was not obvious, and on the day after seeding, there was no difference in the number of adherent cells between the two groups.

Cells can respond to the culture surface to which they adhere^[16]. Therefore, their morphology, polarity and function may differ with different coating substrates. RPE-specific markers in hES-RPE cells on three kinds of coating substrates were probed midway (day 10) and the end of the experimental time course (day 20). We found that hES-RPE cells on VTN-N showed polarity and maturation more rapidly than those on other coating substrates. However, at the end of the culture period, the cells were all sufficiently mature, and no significant difference in RPE-specific gene expression levels or cell morphology were observed. Additionally, the speed with which mature hES-RPE cells can be acquired is another advantage of VTN-N.

Phagocytosis is one of the most important functions of RPE cells. After incubation with POS 4h, the percentages of POS-positive cells on each coating substrate were 93.4% (Matrigel), 96.5% (LN-521), and 98.2% (VTN-N), meaning that VTN-N coated hES-RPE cells had a greater phagocytic ability than LN-521 or Matrigel. VTN-N can recognize Arg-Gly-Asp (RGD) motif and bind to $\alpha\beta 5$, which is one of the key proteins involved in RPE phagocytosis^[35]. The vitronectin-binding $\alpha\beta 5$ can localize to focal adhesion and activate focal adhesion kinase (FAK)^[36-38]. This may explain why VTN-N facilitated phagocytosis.

The ultimate goal of hES-RPE cell culture is to obtain high quality hES-RPE cells on a large-scale for clinical applications in treating retinal degenerative diseases. VTN-N had a stable effect on cell adhesion and worked effectively at a low concentration. Thus, it is more cost-effective than LN-521 for large-scale clinical applications.

In conclusion, to obtain optimum quality of hES-RPE cells for clinical transplantation, our results suggested that VTN-N is a superior culture substrate for xeno-free culture and maintenance of hES-RPE as its lower required concentration and ability to promote faster maturation and better phagocytic function. This research may help to establish a standardized culture method with xeno-free and defined coating substrate that supports the clinical use of stem-cell derived RPE cells.

ACKNOWLEDGEMENTS

Foundations: Supported by the National Natural Science Foundation of China (No.81730026; No.81970816); the National Key R&D Program (No.2017YFA0105301); Science and Technology Commission of Shanghai Municipality (No.20Z11900400; No.19495800700).

Conflicts of Interest: Zhu XY, None; Chen YH, None; Zhang T, None; Liu SJ, None; Bai XY, None; Huang XY, None; Jiang M, None; Sun XD, None.

REFERENCES

1 Zhang H, Su BN, Jiao LY, Xu ZH, Zhang CJ, Nie JF, Gao ML, Zhang YV, Jin ZB. Transplantation of GMP-grade human iPSC-derived retinal

pigment epithelial cells in rodent model: the first pre-clinical study for safety and efficacy in China. *Ann Transl Med* 2021;9(3):245.

2 da Cruz L, Fynes K, Georgiadis O, *et al.* Phase 1 clinical study of an embryonic stem cell-derived retinal pigment epithelium patch in age-related macular degeneration. *Nat Biotechnol* 2018;36(4):328-337.

3 Chen KG, Mallon BS, McKay RD, Robey PG. Human pluripotent stem cell culture: considerations for maintenance, expansion, and therapeutics. *Cell Stem Cell* 2014;14(1):13-26.

4 Sugino IK, Gullapalli VK, Sun Q, *et al.* Cell-deposited matrix improves retinal pigment epithelium survival on aged submacular human Bruch's membrane. *Invest Ophthalmol Vis Sci* 2011;52(3):1345-1358.

5 Takahashi K, Tanabe K, Ohnuki M, Narita M, Ichisaka T, Tomoda K, Yamanaka S. Induction of pluripotent stem cells from adult human fibroblasts by defined factors. *Cell* 2007;131(5):861-872.

6 Yap L, Tay HG, Nguyen MTX, Tjin MS, Tryggvason K. Laminins in cellular differentiation. *Trends Cell Biol* 2019;29(12):987-1000.

7 Pennington BO, Clegg DO, Melkoumian ZK, Hikita ST. Defined culture of human embryonic stem cells and xeno-free derivation of retinal pigmented epithelial cells on a novel, synthetic substrate. *Stem Cells Transl Med* 2015;4(2):165-177.

8 Rowland TJ, Blaschke AJ, Buchholz DE, Hikita ST, Johnson LV, Clegg DO. Differentiation of human pluripotent stem cells to retinal pigmented epithelium in defined conditions using purified extracellular matrix proteins. *J Tissue Eng Regen Med* 2013;7(8):642-653.

9 Braam SR, Zeinstra L, Litjens S, Ward-van Oostwaard D, van den Brink S, van Laake L, Lebrin F, Kats P, Hochstenbach R, Passier R, Sonnenberg A, Mummery CL. Recombinant vitronectin is a functionally defined substrate that supports human embryonic stem cell self-renewal via $\alpha 5 \beta 1$ integrin. *Stem Cells* 2008;26(9):2257-2265.

10 Rodin S, Antonsson L, Niaudet C, *et al.* Clonal culturing of human embryonic stem cells on laminin-521/E-cadherin matrix in defined and xeno-free environment. *Nat Commun* 2014;5:3195.

11 Ilmarinen T, Thielges F, Hongisto H, Juuti-Uusitalo K, Koistinen A, Kaarniranta K, Brinken R, Braun N, Holz FG, Skottman H, Stanzel BV. Survival and functionality of xeno-free human embryonic stem cell-derived retinal pigment epithelial cells on polyester substrate after transplantation in rabbits. *Acta Ophthalmol* 2019;97(5):e688-e699.

12 McGill TJ, Bohana-Kashtan O, Stoddard JW, *et al.* Long-term efficacy of GMP grade xeno-free hESC-derived RPE cells following transplantation. *Transl Vis Sci Technol* 2017;6(3):17.

13 Plaza Reyes A, Petrus-Reurer S, Antonsson L, *et al.* Xeno-free and defined human embryonic stem cell-derived retinal pigment epithelial cells functionally integrate in a large-eyed preclinical model. *Stem Cell Reports* 2016;6(1):9-17.

14 Abdal Dayem A, Lee S, Choi HY, Cho SG. The impact of adhesion molecules on the *in vitro* culture and differentiation of stem cells. *Biotechnol J* 2018;13(2):1700575.

15 Gattazzo F, Urciuolo A, Bonaldo P. Extracellular matrix: a dynamic microenvironment for stem cell niche. *Biochim Biophys Acta* 2014;1840(8):2506-2519.

- 16 Wei M, Li S, Le W. Nanomaterials modulate stem cell differentiation: biological interaction and underlying mechanisms. *J Nanobiotechnology* 2017;15(1):75.
- 17 Okeyo KO, Kurosawa O, Yamazaki S, Oana H, Kotera H, Nakauchi H, Washizu M. Cell adhesion minimization by a novel mesh culture method mechanically directs trophoblast differentiation and self-assembly organization of human pluripotent stem cells. *Tissue Eng Part C Methods* 2015;21(10):1105-1115.
- 18 Buchholz DE, Pennington BO, Croze RH, Hinman CR, Coffey PJ, Clegg DO. Rapid and efficient directed differentiation of human pluripotent stem cells into retinal pigmented epithelium. *Stem Cells Transl Med* 2013;2(5):384-393.
- 19 Foltz LP, Clegg DO. Rapid, directed differentiation of retinal pigment epithelial cells from human embryonic or induced pluripotent stem cells. *J Vis Exp* 2017;(128):56274.
- 20 Hazim RA, Volland S, Yen A, Burgess BL, Williams DS. Rapid differentiation of the human RPE cell line, ARPE-19, induced by nicotinamide. *Exp Eye Res* 2019;179:18-24.
- 21 Miyazaki T, Futaki S, Suemori H, Taniguchi Y, Yamada M, Kawasaki M, Hayashi M, Kumagai H, Nakatsuji N, Sekiguchi K, Kawase E. Laminin E8 fragments support efficient adhesion and expansion of dissociated human pluripotent stem cells. *Nat Commun* 2012;3:1236.
- 22 Finnemann SC, Bonilha VL, Marmorstein AD, Rodriguez-Boulan E. Phagocytosis of rod outer segments by retinal pigment epithelial cells requires alpha(v)beta5 integrin for binding but not for internalization. *Proc Natl Acad Sci U S A* 1997;94(24):12932-12937.
- 23 Jiang M, Esteve-Rudd J, Lopes VS, Diemer T, Lillo C, Rump A, Williams DS. Microtubule motors transport phagosomes in the RPE, and lack of KLC1 leads to AMD-like pathogenesis. *J Cell Biol* 2015;210(4):595-611.
- 24 Müller C, Charniga C, Temple S, Finnemann SC. Quantified F-actin morphology is predictive of phagocytic capacity of stem cell-derived retinal pigment epithelium. *Stem Cell Reports* 2018;10(3):1075-1087.
- 25 Marmorstein AD, Marmorstein LY, Rayborn M, Wang X, Hollyfield JG, Petrukhin K. Bestrophin, the product of the Best vitelliform macular dystrophy gene (VMD2), localizes to the basolateral plasma membrane of the retinal pigment epithelium. *Proc Natl Acad Sci U S A* 2000;97(23):12758-12763.
- 26 Jin M, Li S, Moghrabi WN, Sun H, Travis GH. Rpe65 is the retinoid isomerase in bovine retinal pigment epithelium. *Cell* 2005;122(3):449-459.
- 27 Rachel RA, Mason CA, Beermann F. Influence of tyrosinase levels on pigment accumulation in the retinal pigment epithelium and on the uncrossed retinal projection. *Pigment Cell Res* 2002;15(4):273-281.
- 28 Bharti K, Liu W, Csermely T, Bertuzzi S, Arnheiter H. Alternative promoter use in eye development: the complex role and regulation of the transcription factor MITF. *Development* 2008;135(6):1169-1178.
- 29 Valencia JC, Watabe H, Chi A, et al. Sorting of Pmel17 to melanosomes through the plasma membrane by AP1 and AP2: evidence for the polarized nature of melanocytes. *J Cell Sci* 2006;119(Pt 6):1080-1091.
- 30 Forest DL, Johnson LV, Clegg DO. Cellular models and therapies for age-related macular degeneration. *Dis Model Mech* 2015;8(5):421-427.
- 31 Mehat MS, Sundaram V, Ripamonti C, et al. Transplantation of human embryonic stem cell-derived retinal pigment epithelial cells in macular degeneration. *Ophthalmology* 2018;125(11):1765-1775.
- 32 Schwartz SD, Regillo CD, Lam BL, et al. Human embryonic stem cell-derived retinal pigment epithelium in patients with age-related macular degeneration and Stargardt's macular dystrophy: follow-up of two open-label phase 1/2 studies. *Lancet* 2015;385(9967):509-516.
- 33 Hongisto H, Ilmarinen T, Vattulainen M, Mikhailova A, Skottman H. Xeno- and feeder-free differentiation of human pluripotent stem cells to two distinct ocular epithelial cell types using simple modifications of one method. *Stem Cell Res Ther* 2017;8(1):291.
- 34 Lu HF, Chai C, Lim TC, Leong MF, Lim JK, Gao S, Lim KL, Wan AC. A defined xeno-free and feeder-free culture system for the derivation, expansion and direct differentiation of transgene-free patient-specific induced pluripotent stem cells. *Biomaterials* 2014;35(9):2816-2826.
- 35 Yu C, Muñoz LE, Mallavarapu M, Herrmann M, Finnemann SC. Annexin A5 regulates surface $\alpha\beta 5$ integrin for retinal clearance phagocytosis. *J Cell Sci* 2019;132(20):jcs.232439.
- 36 Kim JP, Zhang K, Chen JD, Kramer RH, Woodley DT. Vitronectin-driven human keratinocyte locomotion is mediated by the alpha v beta 5 integrin receptor. *J Biol Chem* 1994;269(43):26926-26932.
- 37 Zuidema A, Wang W, Kreft M, Molder LT, Sonnenberg A. Mechanisms of integrin $\alpha\beta 5$ clustering in flat clathrin lattices. *J Cell Sci* 2018;131(21):jcs.221317.
- 38 Keasey MP, Jia CH, Pimentel LF, Sante RS, Hagg T. Blood vitronectin is a major activator of LIF and IL-6 in the brain through integrin-FAK and uPAR signaling. *J Cell Sci* 2017;131(3):jcs.202580.